An Improved Chirp Typed Blind Watermarking Algorithm Based on Wavelet and Fractional Fourier Transform

Wang Dian-hong, Li Dong-ming, Yan Jun, Chen Fen-xiong
Electromechanical institute of China University of Geosciences, Wuhan China 430074
E-mail： universelidongming@gmail.com

Abstract

Spatial domain-based Chirp signal watermark can be detected blindly through the Fractional Fourier Transform in the transform domain. The purpose of this paper is to outline the state of the research of wavelet transform domain-based watermark and to propose an improved algorithm towards it. With regard to the later we first analyze the optimum order of the Hermite matrix for the computation of Direct Discrete Fourier Transform. Then we focus on Chirp signals hiding in the low frequency band of the host image in Wavelet domain. Results of the experiments revealed that our improved blind watermark detection algorithm is more robust comparing with conventional spatial algorithm. In addition, it detects the Chirp watermark rapidly.

Index Terms—Wavelet Transform, Fractional Fourier Transform, Digital watermarking, Chirp signal watermark

1. Introduction

Digital watermarking was a new technology that could be used in copyright protection, source authentication and integrity in network[1-5]. Two types of commonly used watermark embedding algorithms works in spatial domain and in transform domain respectively. The shortcoming of spatial watermarking algorithm, which directly embed information into the spatial domain of digital media, is that it is not robust enough to image processing. On the other hand, transform domain watermarking algorithms, which hide information in the transform domain, attract more attention of recent study for its excellent stability and robustness. As one method work in the transform domain, the Chirp Watermarking was proposed by Stnkovic S in 2001. Chirp signal can be focused to a point in FrFT (Fractional Fourier Transform) domain [6-9]. In literature [10] a two-dimensional signal watermarking algorithm is proposed. Chirp signal was embedded into host image, and then the Radon-Wigner transform was performed on the host image. A higher peak value in the transform domain than the threshold value will indicates the existence of watermarking. But if the watermark is a multi-chirp signal, the nonlinear transform will brought in cross-term. In literature [11], a Chirp signal was embedded into the Fractional Fourier domain, and then inverse FRFT was used to get the watermarked image. However, error in the discrete computation of FrFT means that the inverse FRFT can not restore the origin signal exactly. Obviously, embedding the watermark into the Fractional Fourier domain will reduce accuracy of the restoration, therefore reduce the transparency of the watermark. In literature [12, 13], a two-dimensional chirp signal was embedded into the spatial domain of the host image, then the watermark was detected by checking the peak coefficients in the Fractional Fourier domain at certain order. The problem is that adding watermark into spatial domain of the host image cannot resist signal-processing attacking, not to mention that the data of the watermark is small. To enhance the anti-attack capability of the watermark, a Fractional Fourier Domain algorithm is proposed in this paper. First, we analyze the Hermite matrix operator and selected the reasonable optimum order for computation in Direct Discrete FrFT. Then we add two-dimensional Chirp signal into low-frequency band of the host image in wavelet domain. Last, we detect the watermark in the FrFT domain of the low-frequency wavelet coefficients of the host image. Simulation experiments indicate that the improved watermarking algorithm has effectively improved the anti-attack capability of the watermark.

2. FRFT Computation and error analysis

The pth-order FRFT of a function x(t) is defined as

$$X_p(u) = \int_{-\infty}^{+\infty} x(t) K_p(t,u) dt \qquad (1)$$

Where the kernel is

0-7695-2929-1/07 $25.00 © 2007 IEEE
DOI 10.1109/ICIG.2007.38

$$K_p(t,u)=\begin{cases}\sqrt{\dfrac{1-j\cot\alpha}{2\pi}}e^{(j\frac{t^2+u^2}{2}\cot\alpha-tu\csc\alpha)}, & \alpha\neq n\pi\\ \delta(t-u), & \alpha=2n\pi\\ \delta(t+u), & \alpha=\alpha=(2n+1)\pi\end{cases}$$

$$=\sum_{n=0}^{\infty}e^{jn\alpha}H_n(t)H_n(u) \tag{2}$$

here j is the imaginary unit, and $n\in Z$. When the order P=2n or p=2n+1, the kernel should be $\delta(u-t)$ or $\delta(u+t)$ respectively. It must be pointed out that the kernel is a continuous function of P in the case of generalized function, that means $\lim_{p\to 2n} K_p = K_{2n}$, and $\lim_{p\to 2n+1} K_p = K_{2n+1}$

$H_n(t)$ is a Hermite function:

$$H_n(t)=\frac{1}{\sqrt{2^n n!\sqrt{\pi}}}h_n(t)e^{-\frac{t^2}{2}} \tag{3}$$

$h_n(t)$ is a n^{th} order Hermite polynomial: $h_n(t)=(-1)^n e^{t^2}\dfrac{d^n}{dt^n}(e^{-t^2})$.

According to literature [9], we use direct FrFT computation as follows:

By formula (1), we can have:

$$X_p(u)=\int_{-\infty}^{+\infty}x(t)K_p(t,u)dt=\sum_{n=0}^{+\infty}H_n(u)(e^{jn\alpha}\int_{-\infty}^{\infty}x(t)H_n(t)dt) \tag{4}$$

The time domain representation of the signal x(t) is confined to the interval $[-\sqrt{\frac{N\pi}{2}},\sqrt{\frac{N\pi}{2}}]$, and its frequency domain representation is also confined to the interval $[-\sqrt{\frac{N\pi}{2}},\sqrt{\frac{N\pi}{2}}]$. Signal x(t) has N point samples, and each sampling interval is $T_s=\sqrt{\frac{2\pi}{N}},U_s=\sqrt{\frac{2\pi}{N}}$, so we get[9]:

$$X_p(u)=\sum_{n=0}^{+\infty}H_n(u)(e^{jn\alpha}\int_{-\infty}^{\infty}x(t)H_n(t)dt)$$

$$=\sum_{n=0}^{N-1}e^{jn\alpha}H_n(u)T_s\overrightarrow{H_n^T}X_N+\sum_{n=N}^{\infty}e^{jn\alpha}H_n(u)T_s\overrightarrow{H_n^T}X_N$$

And in literature [9], it is said that : $\sum_{n=N}^{\infty}e^{jn\alpha}H_n(u)T_s\overrightarrow{H_n^T}X_N\to 0$, when $n\to\infty$. So:

$$X_p(u)=T_s(\sum_{n=0}^{N-1}e^{jn\alpha}\overrightarrow{H_n}\overrightarrow{H_n^T})X_N$$

$$=T_s\bullet H_N D^p H_N^T\bullet X_N=F_p(X_N) \tag{5}$$

Where $D^p=Diag(e^{-j0},e^{-j\alpha},e^{-j2\alpha},\cdots,e^{-j(N-1)\alpha})$

$\overrightarrow{H_n}=[H_{n,-\frac{N-1}{2}},H_{n,-\frac{N-1}{2}+1},\cdots,H_{n,\frac{N-1}{2}}]^T \quad ,n=0,1,2\cdots N-1$.

$\overrightarrow{H_n}$ is N-point vector of the nth order Hermite function, H_N is a $N\times N$ discrete Hermite matrix: $[\overrightarrow{H_1},\overrightarrow{H_2},\cdots,\overrightarrow{H_N}]$, $X_N=[x_{-\frac{N-1}{2}},x_{-\frac{N-1}{2}+1},\cdots,x_{\frac{N-1}{2}}]^T$ is N-point vector of signal x(t).

Unlike what is indicated in literature [9], through the analyzing of the matrix operator F_p we found that if $N>75$, the matrix operator does not work well. We can see spectral norm $\|F_p\|_2$ and spectral condition number $cond(F_p)_2$ of $F_p=T_s\bullet H_N D^p H_N^T$ in figure 1(a) and 1(b), and the restoration precision of inverse FRFT changed with the matrix order N.

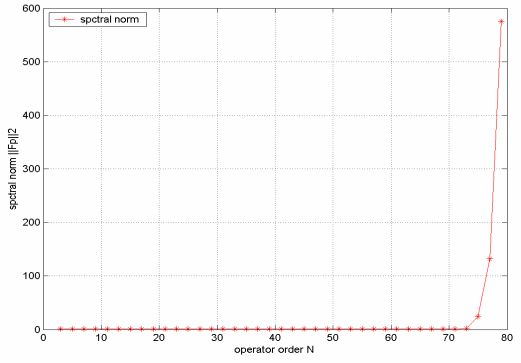

(a)

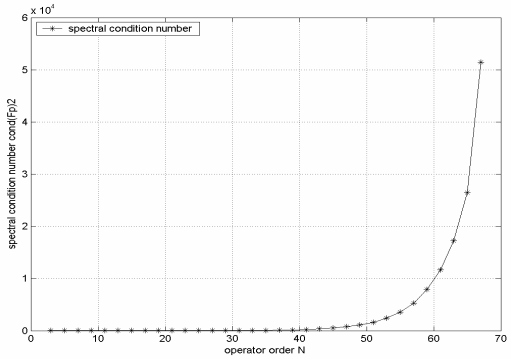

(b)

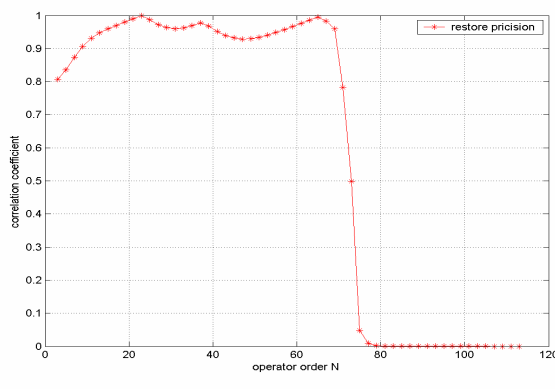

(c)

Figure 1. Operator become infinite, ill-conditioned and irreversible if N>75. (a) Spectral norm ||Fp||2 changed with N. (b) Spectral condition number cond(Fp) 2 changed with N. (c) Precision of inverse FrFT changed with N.

FrRFT is expected to be a linear and finite transform, but from figure 1(a), we can see The Operator become infinite when the order $N > 75$; from figure 1(b), we can see the matrix operator F_p become seriously ill-conditioned, and figure 1(c) indicated that if $N > 75$, the matrix operator F_p could not be used in computation for inverse FrFT. So in this paper, we choose $N = 65$, the spectral norm $\|F_p\|_2 = 1.0553$, which is near to 1.The most important thing in the watermark detection is the computation of FRFT, from formula (5):

$$X_p(u) = T_s \bullet H_N D^p H_N^T \bullet X_N = F_p(X_N)$$

where $T_s = \sqrt{\frac{2\pi}{N}}, D^p = Diag(e^{-j0}, e^{-j\alpha}, e^{-j2\alpha}, \cdots, e^{-j(N-1)\alpha})$,

H_N is a $N \times N$ matrix $[\overrightarrow{H_1}, \overrightarrow{H_2}, \cdots, \overrightarrow{H_N}]$, so we have:

$$X_p(u) = \begin{pmatrix} F_{p,\frac{N-1}{2},\frac{N-1}{2}} & F_{p,\frac{N-1}{2},\frac{N-1}{2}+1} & \cdots & F_{p,\frac{N-1}{2},\frac{N-1}{2}} \\ F_{p,\frac{N-1}{2}+1,\frac{N-1}{2}} & F_{p,\frac{N-1}{2}+1,\frac{N-1}{2}+1} & \cdots & F_{p,\frac{N-1}{2}+1,\frac{N-1}{2}} \\ \vdots & \vdots & \ddots & \vdots \\ F_{p,\frac{N-1}{2},\frac{N-1}{2}} & F_{p,\frac{N-1}{2},\frac{N-1}{2}+1} & \cdots & F_{\frac{N-1}{2},\frac{N-1}{2}} \end{pmatrix} \begin{pmatrix} x_{\frac{N-1}{2}} \\ x_{\frac{N-1}{2}+1} \\ \vdots \\ x_{\frac{N-1}{2}} \end{pmatrix} \quad (6)$$

$X_p(0)$ is the maximum energy concentration in fractional Fourier domain at appropriate order $p = 2\alpha/\pi$:

$$\left|X_p(0)\right| = \left|\sum_{i=-\frac{N-1}{2}}^{\frac{N-1}{2}} F_{0,i} \cdot x_i\right| \le \sum_{i=-\frac{N-1}{2}}^{\frac{N-1}{2}} \left|F_{0,i}\right| \cdot \left|x_i\right|$$

$$= \sum_{i=-\frac{N-1}{2}}^{\frac{N-1}{2}} \left|F_{0,i}\right| = 8.033\,|_{N=65} \quad (7)$$

Therefore, the two-dimensional Chirp signal concentrates on $S_{p_1,p_2}(0,0)$ at appropriate order P_1 and P_2, we have:

$$S_{p_1,p_2}(0,0) = F_{p_1}\{F_{p_2}(I(x,y)\} = F(I(x,y)) = 64.52 \quad (8)$$

On the other hand, we applied FrFT to the low frequency band (LL) of the host image at order $p \ge 1.4$, we found that in the Fractional Fourier domain there is no value bigger than 3 ($S_{p_1,p_2}(0,0) < 3$), so theoretically the peak value in the Fractional Fourier domain of the Chirp signal is about 20 (64.52/3) times bigger than the peak value in Fractional Fourier domain of the low frequency wavelet coefficients of the host image. In practical use, because of the error in the process of the FRFT computation, it is a little bit less than 20, and if we set the embedding intensity $\alpha = 0.1$, the ratio ($\alpha \bullet 64.52/3$) is about 2, and this operation satisfies the transparent requirement of the watermark.

3. Embedding and Extraction of the Watermarking

The two-dimensional Chirp Signal we used was:

$S(x,y) = \sum_{i=1}^{N} A_i \cos(a_i x^2 + b_i y^2)$ where A_i, a_i and b_i were parameters of the Chirp signal, and they could be used as keys in watermarking extraction.

Watermarking embedding process is shown in figure2.

The host image was decomposed into four sub images of different frequency bands: LL, LH, HL, and HH. LL band is the approximation (low frequency) coefficient matrix.

Adding Chirp Signal $S(x,y)$ to the LL band.

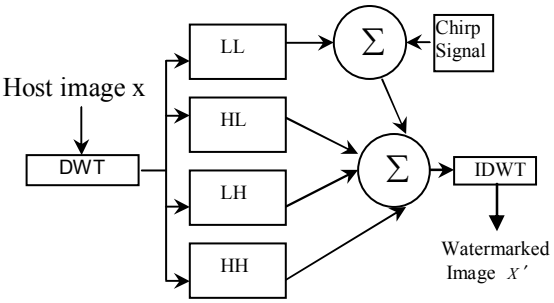

Figure 2. Flows of watermark embedding

Applying Inverse Discrete Wavelet Transform to the four bands, in which the LL band had been modified by Chirp Signal.

Watermarking extraction process is shown in figure3.

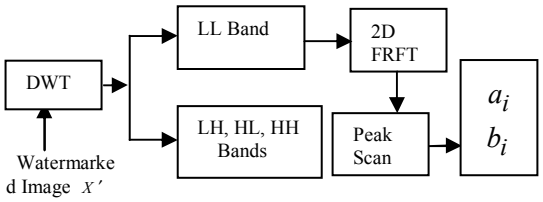

Figure 3. Flows of watermark extraction

Applying DWT(Discrete Wavelet Transform) to watermarked image X', and we get LL band.

Applying FrFT (Fractional Fourier Transform) to LL band at order p from 1 to 2, and the step size is 0.005.

Scanning and recording max value $\max\left|X_{p_1,p_2}(u,v)\right|$ in each Fractional Fourier domain in step (2).

Plotting a graph with coordinate p and $\max\left|X_{p_1,p_2}(u,v)\right|$. The local peaks in the graph indicate the existence of the embedded Chirp Signal watermark.

4. Experiment results

To visualize the digital watermarking effect, we implemented our algorithm on the "wbarb" host image with two-dimensional watermark. The experimental results are illustrated in figure 4 through figure 8.

The frequency of the Chirp signal we used as watermark was $a_1 = b_1 = 0.015$, $a_2 = b_2 = 0.06$, the theoretical concentration order is $p_1 = p_2 = 1.21$ and $p_1 = p_2 = 1.58$, the wavelet used in the algorithm was "db10", the amplitude $A_1 = A_2 = 1$, the embedding intensity was $\alpha = 0.05$, the scanning step was 0.005. The PSNR between the host image and the image after embedding was $PSNR = 48.8173$, which ensured the invisible of the watermark.

(a)

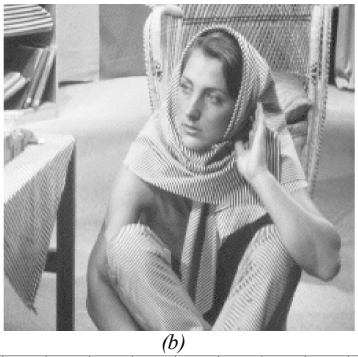

(b)

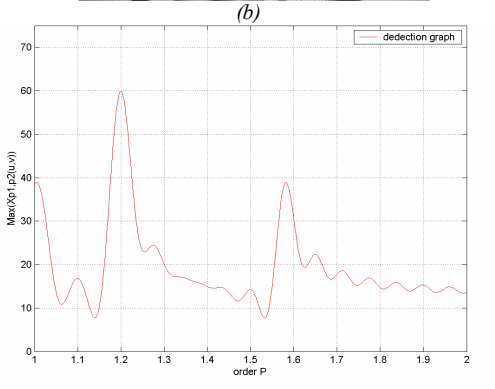

(c)

Figure 4. Figure 4(a) is the "wbarb" host image; Figure 4(b) is the watermarked image; Figure 4(c) is the FrFT detection graph at order changed from 1 to 2.This graph has two local peaks related to the watermark's two parameters a_i and b_i.

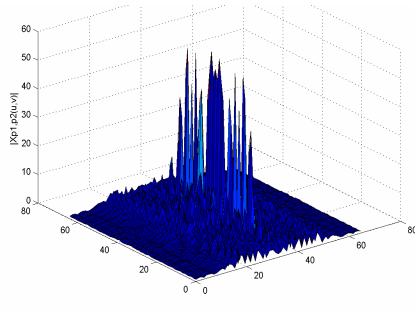

(a)

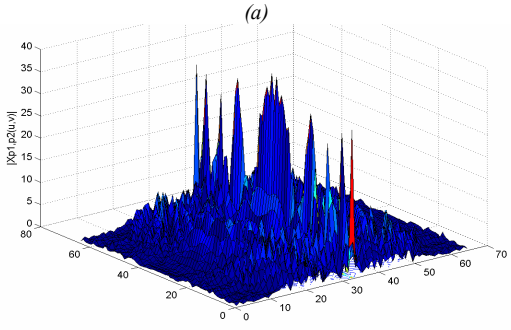

(b)

Figure 5. Figure (a) and figure (b) were the concentration of Chirp signal in the Fractional Fourier domain at order P1=P2=1.21 and P1=P2=1.58 separately.

(1) Cropping attack

(a)

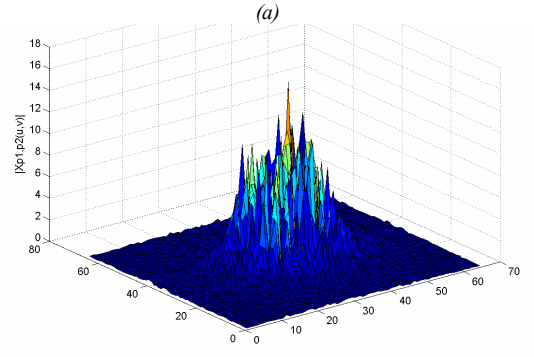

(b)

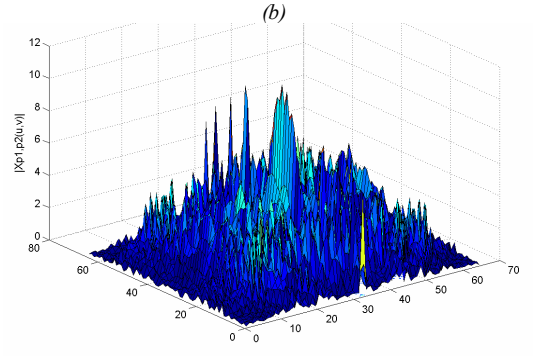

(c)

Figure 6. Figure (a) was the watermarked image after cropping 30%, figure (b) and figure (c) were the concentration of Chirp signal in the Fractional Fourier domain at order P1=P2=1.21 and P1=P2=1.58 separately.

(2) Rotation attack

(a)

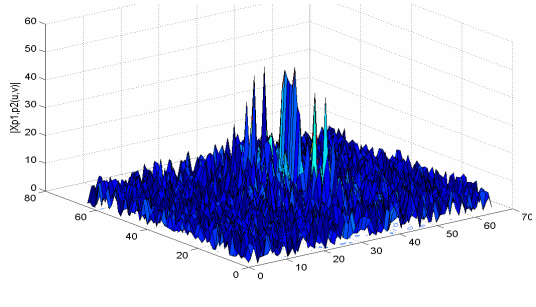

(b)

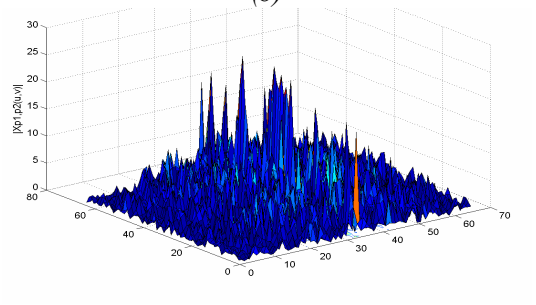

(c)

Figure 7. Figure (a) was the watermarked image after rotation 200, figure (b) and figure (c) were the concentration of Chirp signal in the Fractional Fourier domain at order P1=P2=1.21 and P1=P2=1.58 separately.

(3) Gaussian noise attack

(a)

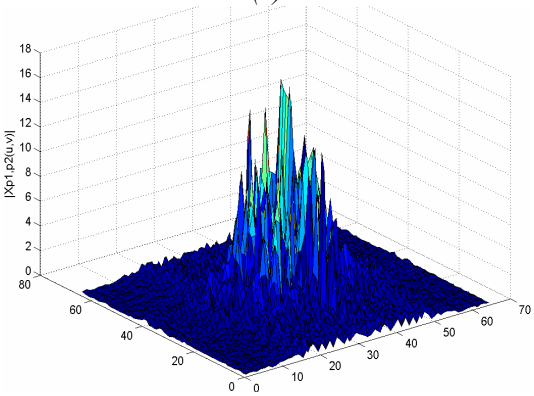

(b)

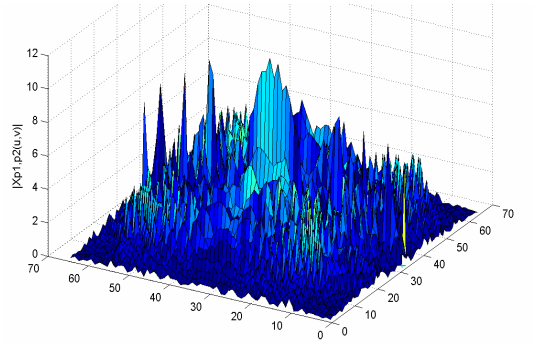

(c)

Figure 8. Figure (a) was the watermarked image after attacked by Gaussian noise with mean=0,variance=0.05, figure (b) and figure (c) were the concentration of Chirp signal in the Fractional Fourier domain at order P1=P2=1.21 and P1=P2=1.58 separately.

Table 1.Anti-attack comparison between watermark embedding into spatial domain and low frequency band of wavelet domain

embedding intensity α	no attack	Gsussian noise	compression JPEG2000 (32：1)
	$p_1, p_2 / p_1', p_2'$	$p_1, p_2 / p_1', p_2'$	$p_1, p_2 / p_1', p_2'$
0.05	1.00,√1.21,1.58	1.00,√1.20,1.55	1.00,√1.20,1.57
0.06	1.15,√1.21,1.58	1.00,√1.20,1.56	1.05,1.48/1.21,1.58
0.07	1.17,1.54/1.21,1.58	1.10,1.48/1.21,1.56	1.08,1.50/1.21,1.58
0.08	1.18,1.55/1.21,1.58	1.10,1.48/1.21,1.57	1.11,1.52/1.21,1.58
0.09	1.20,1.55/1.21,1.58	1.13,1.50/1.21,1.58	1.14,1.51/1.21,1.58
0.10	1.21,1.57/1.21,1.58	1.15,1.50/1.21,1.58	1.17,1.50/1.21,1.58
embedding intensity α	rotated 45^0	rotated 25^0	cropping (30%)
	$p_1, p_2 / p_1', p_2'$	$p_1, p_2 / p_1', p_2'$	$p_1, p_2 / p_1', p_2'$
0.05	1.00,√1.20,1.56	1.00,√1.20,1.56	1.00,√1.20,1.54
0.06	1.00,√1.20,1.57	1.00,√1.21,1.56	1.00,√1.20,1.56
0.07	1.00,√1.21,1.57	1.00,√1.21,1.57	1.00,√1.20,1.56
0.08	1.10,1.44/1.21,1.58	1.07,1.44/1.21,1.57	1.06,√1.21,1.56
0.09	1.12,1.40/1.21,1.58	1.10,1.43/1.21,1.58	1.05,√1.21,1.57
0.10	1.15,1.42/1.21,1.58	1.10,1.44/1.21,1.58	1.05,1.40/1.21,1.58

5. Conclusion

We have researched which is the best order of the Hermite matrix used in the computation of the FrFT, and embedded Chirp signal into low frequency band of host image in wavelet domain, which performed better than the conventional spatial-embedding method. The watermark detection was proceeding in the Fraction Fourier domain, and it doesn't need the original image. The next step of research should focus on the location tamper and the design of special meaning watermark.

6. References

[1] Wong P W. "A public watermark for image verification and authentication," In: Proc Int conf on Image Processing, Chiacgo,Illinois,1998.

[2] Bender W, Gruhl D, "Morimoto N. Technique for data hiding," Technical Reprt, MIT Media Lab, 1994.

[3] Pitas I. " Method for signature casting on digital images," In Proc Int Conf on Image Processing, Lausanne, Switzerland, 1996

[4] Pitas I, Kaskalis T H. "Apply signatures on digital images." In: NesMsrmaros,Greece,Proc IEEE Workshop Nonlinear Image and Signal

[5] Lufs B. Almeida. "The fractional Fourier transform and time2frequencyrepresentations," IEEE Transactions on Signal Processing,1994 ,42(11) :3084 - 3091.

[6] B.Santhanam and J.H. McClellan. "The discrete rotational Fourier transform," IEEE Transactions on Signal Processing ,1996 ,42 (4) :994 - 998.

[7] Haldum M. Ozaktas ,Orhan Arikan ,M. Alper Kutay and Gozde Bozdag2i . "Digital Computation of the Fractional Fourier Transform," IEEE Transactons on Signal Processing,1996,44(9):2141-2150.

[8] Soo2Chang Pei ,Min2Hung Yeh and Chien2Cheng Tseng. "Discrete fractional fourier transform based on orthogonal projections," IEEETransactions on Signal Processing,1999,47(5):1335-1347.

[9] Ping Xian-jun, Ta0 Ran ,Zhou Si-yong ,et al. "A Novel Fast Algorithm for Fractional Fourier Transform," Acta Electronica Sinica. 2001,29(3):406-408

[10] Stankovic S, Djurovic I, Pitas I. "Watermarking in the Space/Spatial-Frequency Domain Using Two-Dimensional Radon- Wigner Distribution,".IEEE Trans on Image Processing, 2001.10(4):650－65812.

[11] Liu Zheng-jun, Zhao Hai-fa, Zhu Bang-he, et al. "Fractional Fourier Domain Digital Watermarking,". ACTA PHOTONICA SINICA. 2002.32(3): 332-335

[12] Zhang Feng, Mu Xiao- min, Yang Shou- yi, et al. "Chirp Typed Blind Watermarking Algorithm Based on Fractional Fourier Transform," Computer Engineering and Applications. 2006(27): 57-61

[13] Zhu Chun-hua1, MU Xiao-ming, Zhang Feng. "New Watermark Algorithm Based on Modified Chirp-fourier Transform," Computer Engineering. 2006.32(17): 213-215